RSC Advances

ROYAL SOCIETY OF CHEMISTRY

www.rsc.org/advances

A table of contents entry

A low melting point bismuthate glass was developed for bonding SiC_p/Al composite, and the novel SiC_p/Al composite-glass material was prepared.

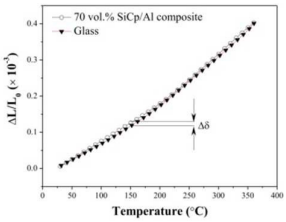

Journal Name

ARTICLE

Preparation of SiC_p/Al composite-bismuthate glass material and their application in mirror blank

Received 00th January 20xx,
Accepted 00th January 20xx

DOI: 10.1039/x0xx00000x

www.rsc.org/

S. G. Qu,[a] H. S. Lou,[a,b,*] X. Q. Li,[a] and T. R. Kuang[a]

In this work, a low melting point bismuthate glass was developed for bonding on the 70 vol.% SiC_p/Al composite surface, and the novel SiC_p/Al composite-glass material was prepared. The measured data of mechanical properties showed that the shear strength of the composite-glass material achieved 5.44 MPa. The morphology was characterized using field emission gun scanning electron microscope (FEGSEM), X-ray photoelectron spectroscopy (XPS) and Line-scan. The mutual solubility between the glass and the composite formed an interface layer with about 2 μm in thickness. The bond strength of glass-matrix was greater than that of glass-particle. It can be attributed to the chemical bonding between the glass and the matrix. During bonding, a strong chemical bond at the interface was resulted from the incorporation the oxide film on the composite surface into the glass. The metallic bonding of the matrix was gradually substituted for the ionic-covalent bonding of the glass within the interface. In the local region, the Bi ions in the glass gained the free electrons from the Al metal atoms of the composite, producing the precipitates of Bi atoms on the composite surface which formed an interlocking composite-glass structure. The polished composite-glass material achieved 0.05λ at 632.8-nm p-v surface error, showing that the novel material was suitable for application of mirror blank.

Introduction

Selecting optical grade SiC_p/Al composite with high SiC content as space mirror material is propitious to promote the integration of the mirror and its supporting structure. Thus, more attention has been placed on simplifying the mirror systems and lowering cost. Guo et al.[1] studied the effects of materials on the mirror design by finite element analysis, and they found the figure error PV value of SiC_p/Al mirror could satisfy the requirements of optical system. Zhang et al.[2] prepared plane mirror with open back lightweight structure, thereby reducing cost. However, due to the high hardness and low plasticity, it is difficult to machine this kind of materials to achieve high surface micro-roughness.[3] Most of the research work carried out in this field focused on electroless Ni deposition on SiC_p/Al composite.[4] At present, glassy coating, as a surface modification technique to bond the glass on the SiC_p/Al composite surface, has been attracted more interest because of the higher polishability of surface can be obtained by using the novel SiC_p/Al composite-glass material.[5-7] In order to obtain the novel SiC_p/Al composite-glass material with high bonding strength, the glass must meet a number of requirements. For example, its thermal expansion coefficient (CTE) should match that of the SiC_p/Al composite to prevent the formation of tensile in the glass after cooling from the bonding temperature.[5, 8] In addition, the melting point of the matrix of SiC_p/Al composite is relatively low (≤ 660 □). High bonding temperature increases the risk of melting the matrix, resulting in the formation of cavities and degrading the matrix soundness.[9] Therefore, the bonding temperature should be controlled within a specified temperature range. Furthermore, the bonding strength of SiC_p/Al composite-glass components plays an important role on its reliability. Chanmuang et al.[10] prepared the borosilicate glass-to-Kovar joint by bonding glass to the alloy, and the joint has a bonding strength of 4.3 MPa. However, to the best of our knowledge, very few studies have been reported the SiC_p/Al composite-glass material for blank mirror application. Therefore, it is still not clear the bonding mechanism of the composite-glass material and also restricted the development of the SiC_p/Al composite-glass material.

The purpose of this study was to develop a low-melting bismuthate glass which meets the main demands of the SiC_p/Al composite-bismuthate glass bonding, and to study the preparation process and property of the novel SiC_p/Al composite-bismuthate glass material for blank mirror application. The bonding mechanism, melting and expansion behaviour, preoxidation of the composite were also investigated.

Experimental

Preparing materials

[a] School of Mechanical and Automotive Engineering, South China University of Technology, Guangzhou 510640, China. E-mail: lou.huashan@mail.scut.edu.cn; Fax: +86-20-8711211; Tel: +86-20-87112948.
[b] Liuzhou Vocational and Technical College, Liuzhou 515007, China.

Chemical compositions of aluminium alloy used in this work are shown in Table 1. The average sizes of SiC particles used in the packing experiment are 45 and 2 μm. The mixtures of two kinds of sizes of SiC particles were ball-mixed in a planetary mixer. Mixed SiC particles were consolidated into a preform. 70 vol.%SiC_p/Al composite was fabricated by squeezing molten aluminium alloy (820 □) to infiltrate into preform under a pressure of 90 MPa.

Table 1 Chemical composition of aluminium alloy

	Composition (wt %)					
	Si	Cu	Mg	Fe	Mn	Al
Aluminium alloy	0.92	1.03	2.28	2.58	0.45	Balanced

Glass with compositions of 72.7Bi_2O_3-15B_2O_3-10BaO-2.3Li_2O was prepared by using reagent grade Bi_2O_3, B_2O_3, BaO and Li_2O. Appropriate amounts (all in wt%) of reagent grade 72.7 wt% Bi_2O_3, 15 wt% B_2O_3, 10 wt% BaO and 2.3 wt% Li_2O were weighed accurately by using an electronic balance. Then, these chemicals were ground to fine powder and blended thoroughly. The mixture in an alumina crucible was melted using an electrical furnace at 1350 □ for 2 h. The purity of the alumina in the alumina crucibleachieved 99.9%.The quenched glass was annealed at 380 □ for 2 h to release thermal stress, and then cooled to room temperature in the furnace. Table 2 shows the properties of the SiC_p/Al composite and the glass.

Table 2 The properties of 70 vol.% SiC_p/Al composite and the glass

	Elastic modulus (GPa)
SiC_p/Al composite	192.6[a]
glass	72.6[a]

[a] Experimental data.

The bonding SiC_p/Al composite-glass experiment was conducted in an oxygen atmosphere at 565 □ for 20 min, and then the SiC_p/Al composite-glass material was annealed at 380 □ for 2 h to release the thermal stresses.

Characterization

The endothermic temperature of the composite was measured by using a Differential Scanning Calorimetry (DSC).[11] The glass transition temperature, T_g, the onset of crystallization peak T_x and the melting temperature T_m were also detected in the DSC. The composite and the glass were machined into cylindrical bars with diameter of 10 mm and length of 25 mm, the top and the bottom of them were ground and polished to guarantee plane-parallel surfaces. The specimens of the composite and the glass were heated between 30□ and 360 □. The thermal expansion coefficient (CTE) of the specimens was measured using a dilatometer 402 TMA F3 with a compressive force of 25-mN. An Instron3365 universal testing system was used to measure the shear strength of the SiC_p/Al composite-glass material. The nominal shear strength τ is calculated as follows:

$$\tau=\frac{F_{max}}{S_{max}} (1)$$

Here F_{max} and S_{max} are the maximum shear and the effective bearing area of the sealed cylindrical sample, respectively. The effective bearing area S_{max} is 7.85 × 10^{-5} m^2.

After the test, the fracture surface and the interface of the SiC_p/Al composite-glass material were observed using a field emission gun scanning electron microscope (FEGSEM). The distribution of elements in the SiC_p/Al composite-glass material was characterized by energy-dispersive X-ray spectroscopy (EDX).[12] The surface electronic states of the SiC_p/Al composite-glass material were analyzed by X-ray photoelectron spectrometer (XPS, Axis Ultra DLD electron spectrometer) using monochromes Al Kα radiation (1486.6 eV). The spot size of XPS is about 700 μm × 300 μm, and the spatial resolution is less than 1μm.The spectrometer was calibrated to the carbon C 1s signal at a binding energy of 284.6 eV.[13]

Results and discussion

Melting point

Fig. 1a shows the DSC thermogram of the 70 vol.% SiC_p/Al composite, indicating variation in its thermal response. The curve consists of two endothermic peaks A and B. The endothermic peaks A and B appear at 571.9 □ and 645.5 □, respectively. The chemical composition of the matrix contains the element of iron, and the element of Fe in the matrix can be formed intermetallic compounds.[14] The endothermic peak A at 571.9 □, which was similar to the results reported by Wu et al.[15], could be attributed to the occurrence of the dissolution of $Al(MnFe)_3Si_2$ eutectic phase. The endothermic peak B reveals that the incipient melting of the aluminium alloy took place when the composite was heat-treated at temperature above 645.5 □. The DSC results of the composite suggested that the bonding temperature should not exceed the melting temperature of the $Al(MnFe)_3Si_2$ phase in order to avoid the formation of cavities in the composite.

As seen in Fig. 1b, the onset endothermic peak appears at 360 □, indicated that the transition temperature of the bismuthate glass is around 360 □. The transition temperature of the bismuthate glass can determine the temperature range, which is used to estimate the thermal mismatch stress (σ_{mis}), which induced by the mismatch of

the CTE between the bismuthate glass and 70 vol.% SiC_p/Al composite. During bonding process, when temperature was above 360 □, the bismuthate glass can plastically accommodate the deformation due to the mismatch CTEs between the bismuthate glass and the composite.[16, 17] Therefore, the thermal mismatch stress (σ_{mis}) can be relaxed. After cooling from the bonding temperature, when temperature was below 360 □, the bismuthate glass behaves as an ideal elastic solid. The differences in thermal contraction between the bismuthate glass and the composite can no longer be accommodated, and the influence of the thermal mismatch stress (σ_{mis}) cannot be ignored.[5] The estimation of the thermal mismatch stress (σ_{mis}) will be detail in later. It can be seen that exothermic peak appeared in the range of 415-475□, indicating that the onset crystallization temperature (T_x) of the bismuthate glass is 415 □. The maximum of the exothermic peak (T_p) reveals that the first crystallization temperature is 475 □. The difference of crystallization and glass transition temperature ($\Delta T=T_x-T_g$) of the bismuthate glass notes the crystallization window. The bismuthate glass has a relatively small crystallization window (ΔT = 55 □), implying the instability of the thermal properties.[18] According to the classical theories, the crystallization of the bismuthate glass can be divided two stages, nucleation and subsequent crystal growth. In the crystallization window, crystals are formed within the bismuthate glass. In general, nucleation occurs at about 400 □; and further growth of crystal nuclei occurs when the glass is heat-treated in the temperature 415-475□. The formation of crystals breaks the isotropy of the bismuthate glass and generates the coarse microstructure.[5] It is detrimental to the polishabilityof the bismuthateglass. Therefore, it is necessary to avoid crystallization during bonding SiC_p/Al composite-bismuthate glass. The second endothermic peak of the bismuthate glass occurs at about 560 □ in DSC curve, suggesting that the bismuthate glass with compositions of $72.7Bi_2O_3$-$15B_2O_3$-10BaO-$2.3Li_2O$ possesses the low melting temperature. The bismuthate glass with a low melting temperature makes it possible to bond SiC_p/Al composite under a low temperature. The bonding temperature is the most important factor in the SiC_p/Al composite-glass bonding process. When the temperature is higher than 571.9 □, the iron intermetallics will melt and is prone to form cavities in the matrix.[14] When the temperature is lower than 560 □, the bond strength of the SiC_p/Al composite-bismuthate glass material is not good due to the weak wetting property.[19] This is the reason why selecting 565 □ as the bonding temperature.

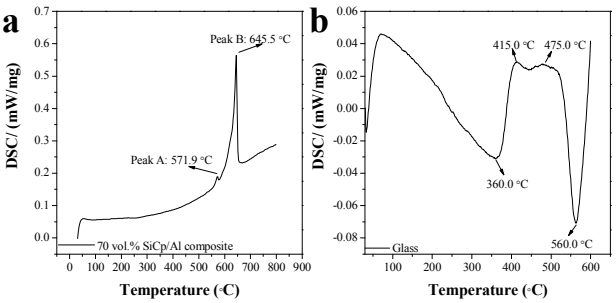

Figure 1 DSC curves of (a) the 70 vol.% SiC_p/Al composite, (b) the glass.

Expansion behaviour

The thermal expansion curves between 30 □ to 360 □ of the glass and the composite are shown in Fig. 2. The CTEs of the glass and the composite increased almost linearly with the increase of temperature. The thermal expansion curve of the glass is very similar with that of the composite, indicating that the glass and the composite have the similar expansion rates. Moreover, it should be noted that at a given temperature, the CTE of the glass is lower than that of the composite. It means that the glass will be in compression during cooling process.[5] As the glass has a better compression than tension[20], the compressive stress in the glass is beneficial to avoid crack. In Fig. 2, the differential thermal expansion rate between the bismuthate glass and SiC_p/Al composite, $\Delta\delta$, is used to quantify the relative displacement of the two curves at a given temperature. The maximum $\Delta\delta$ of about 6.76×10^{-6} was observed at 150 □. McLellan et al. thought that the $\Delta\delta$ should not exceed a value of 5×10^{-4} to obtain a satisfactory seal.[5, 21] Because the maximum $\Delta\delta$ is much less than 5×10^{-4}, the bismuthate glass and 70 vol.% SiC_p/Al composite can form the matched bonding.

The thermal mismatch stress, $\sigma_{mis,}$ plays an important role in the life of composite-bismuthate glass material. The maximum thermal mismatch stress, σ_{mis}, can be calculated by using the following expression:

$$E_g\Delta\delta \le \sigma_{mis} \le E_c\Delta\delta \quad (2)$$

Here E_g and E_c are the elastic modulus of the glass and the composite, respectively (See Table 2 for the elastic modulus of the glass and the composite). Introducing the $\Delta\delta$, E_g and E_c into Equation (2), the maximum thermal mismatch stress σ_{mis} is in the range of 0.49-1.3 MPa. The maximum thermal mismatch stress, σ_{mis}, is much less than 10 MPa, indicating that the SiC_p/Al composite-material can remain hermetic over its service lifetime.[5]

As mirror materials, the $\Delta\delta$ determines the dimensional stability of the mirror. For the mirror with the thickness *H* mm glass layer, the local dimension variation, $\Delta\zeta$, induced by the $\Delta\delta$ can be calculated by:

$$\Delta\zeta = H \times \Delta\delta \quad (3)$$

According to the equation (3), when the H is 1 mm, the $\Delta\zeta$ is less than 6.76×10^{-6} mm. It means that the effect of the $\Delta\zeta$ on the profile accuracy of the mirror only achieves the levels of nanometer. When the bismuthate glass and SiC_p/Al composite both present isotropic homogeneity, the effect of the $\Delta\zeta$ on the profile accuracy of the mirror may be neglected. The validity of the assumption will be verified in later.

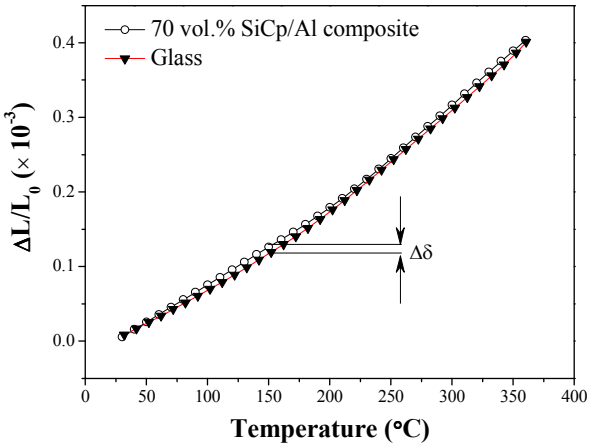

Figure 2 Comparing the thermal expansion behavior of 70 vol.% SiC_p/Al composites and glass obtained from 30 □ to 360 □

Preoxidation of the composite

The reliability of the composite-glass bond is related with the oxide film thickness. When the composite is over-oxidized, it causes that the thick oxide layer easily detaches from the composite surface. When the oxide film is too thin, the wetting property between the glass and the composite would decrease, and not get bonding.[19] During bonding, it is well known that the oxide layer with 2-3 μm can avoid a direct contact between the glass and the composite [20], and the dissolution of this oxide layer can also improve the wetting property.[10] Therefore, the oxide film thickness on the composite is a concern. According to other researchers report, we know that temperature and bonding time plays an important role in the oxide film thickness during bonding.[19]

In our work, we prepared the SiC_p/Al composite-glass material in an oxygen atmosphere at 565 □ for 20 min. As shown in Fig. 3, we can see the backscattered electron image of the cross-section of the composite after preoxidation at 565 □ for 20 min. A certain layer made of Al_2O_3 was grown on the composite surface and the oxide film thickness is in the range of 2-3 μm. The result indicates that at 565 □ for 20 min under an oxygen atmosphere, the oxide film with suitable thickness was successfully formed on the composite surface during the initial stages of bonding composite-glass, thus ensuring the quality of the new materials.

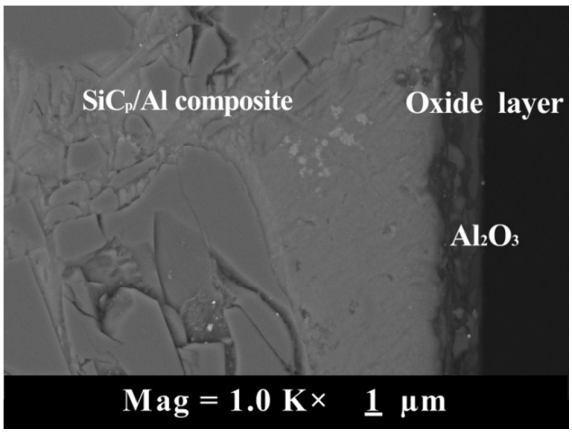

Figure 3 Micrograph (backscattered electrons) of the composite after preoxidation at 565℃ for 20min.

Mirror blank and property

Fig. 4a presents the mirror blank with diameter of 75 mm and thickness of 15 mm, which was grinded and polished with CeO_2 polishing powder.The bismuthate glass layer appears bright glittering and translucent, no cracks and crystals are found in the blank. The results indicate that the process of bonding composite-bismuthate glass is perfect. During bonding, composite and glass were directly heated at 565 □ for 20min, the formation of crystal nuclei in the glass was effectively inhibited due to the short nucleation time; then SiC_p/Al composite-glass material was cooled quickly through crystallization window and annealed at 380 □ for 2 h, the crystal growth was prevented because the annealing temperature is less than the onset crystallization temperature T_x (415 □).

The wavefront error of the mirror blank was measured by Zygo interferometer, as shown in Fig. 4b. The profile accuracy of the mirror achieves 0.1λ at 632.8-nm p-v surface error, and the root-mean-square roughness of the mirror achieves 0.016λ at 632.8-nm. The results indicate that the novel SiC_p/Al composite-glass materials are suitable for the preparation of mirror, and the hypothesis, which the effect of the $\Delta\zeta$ on the profile accuracy of the mirror can be neglected, is tenable.

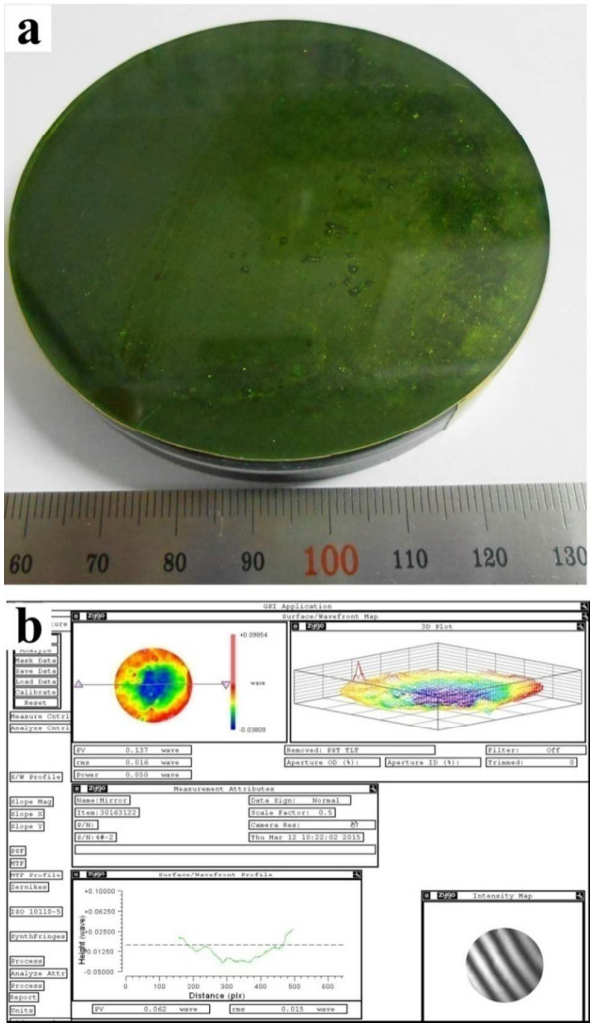

Figure 4 (a) Mirror blank, (b) Wavefront error of mirror.

Fig. 5a shows a low magnification (× 500) cross-sectional observation of the composite-glass material. The micrograph presents a relatively good bonding between the composite and the glass. No crack formation along the composite-glass interface can be found. Meanwhile, several spherical inclusions with a diameter less than 20 μm are noted near the interface.

At higher magnification, it can be clearly observed in Fig. 5b that the inclusion contains amounts of 2 μm SiC particles. The inclusions can be attributed to the detachment of fine particles from the composite surface during bonding process. The wetting property of the local region is very poor owing to the aggregation of fine particles.[22] The oxide film in the local region may be very thin due to the incomplete infiltration and the small interspacing between the fine particles. At the same time, the local region provides porous path that allows the molten glass to permeate.[19] The excessive corrosion occurred in the local region, causing the depletion of the matrix. It has resulted that a certain amount of fine particles detached from the composite surface. The reason for this phenomenon: the density of the glass (4.5 g/cm^3) is larger than that of SiC particles (3.2 g/cm^3), fine particles are suspended in the glass, and then formed the spherical inclusions. Fig. 5c shows the morphology of the composite-glass material at an even higher magnification (10000 ×). The microstructure can be divided into three regions (Region I is the composite, Region II is the interface, Region III is the glass). As seen in Region II, the thickness of the interface is around 1.5-2 μm. The dendritic phase, bubbles and fine particles are found within the interfacial region. The dendrites are closely intertwined with each other, thereby forming an interlocking structure which can be provided the better adhesion between the glass and the composite. The dendrites can be ascribed to the reaction of a certain metal oxide present in the glass with the matrix.[5] The mechanism will be discussed in the next section. As a chemical product, the bubbles indicate that chemical reactions were involved during bonding. The X-ray emission line scan in Fig. 5c reveals that the element Bi in the glass diffused into the composite, and the element Al in the composite diffused into the glass. The diffusion distance of these elements extends about 4-5 μm in the composite-glass material, suggesting the occurrence of the strong chemical affinity between the glass and the composite.

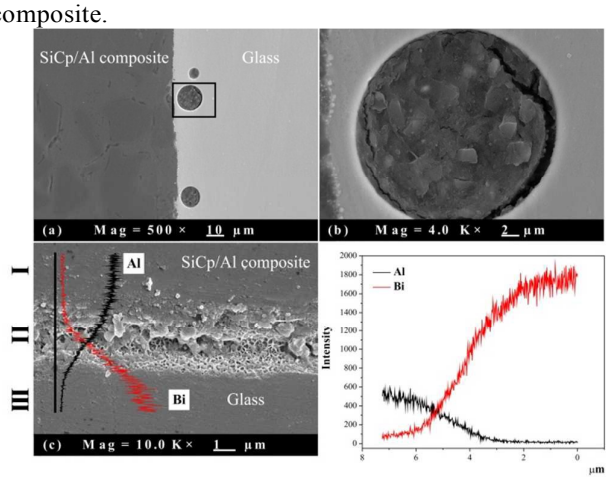

Figure 5(a) The cross-sectional observation of the composite-glass material(b) High magnification image of the framed area in (a), (c)The interface micrograph and X-ray line scans obtained from the composite-glass material.

The maximum shear F_{max} of the composite-glass material is 419 N. Introducing the F_{max} and S_{max} into Equation (1), its shear strength τ can be calculated. The calculated result shows that its shear strength τ can reach 5.34 MPa. Its fracture morphology is shown in Fig. 6a. The fracture induced by the crack propagation through bubbles occurred at the interface. The fracture surface presents large amount of small islands of the glass adhering on the composite surface. The bubbles caused the fracture path to deviate into the glass, thereby forming the river pattern and steps pattern.[23] Meanwhile, it should be noted that

the interfacial debonding took place on the fracture surface. Fig. 6b shows the high magnification image of the debonding region. In the debonding region, the exposed coarse particles are noted. It suggests that the matrix that coated coarse particles may be over-oxidized, and causing that the surface of coarse particles came into contact with the glass during bonding. Under loading, the "pull-off" behaviour of the glass occurred due to the lower bonding strength. At the edge of the debonding region (white arrow), the glass and the matrix were fused together. It shows that the bonding strength between the glass and the matrix is greater than the bonding strength between the glass and SiC particles.

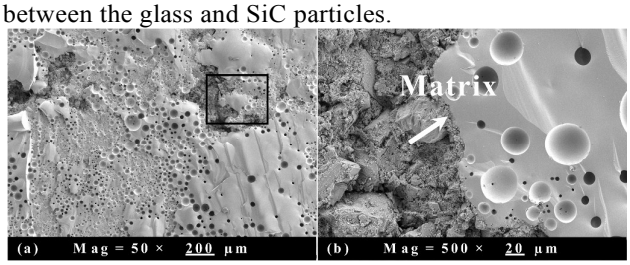

Figure 6 (a) The fracture morphology of the composite-glass material, (b) High magnification image of the framed area in (a).

Bonding mechanism

Fig. 7a shows the Al2p XPS spectra of the composite-glass material recorded from the three regions. In Region I, the peak in the Al spectra represents the metallic state Al^m atoms, and the binding energy of the metal state Al^m atoms is 73.6 eV for Al 2p. In Region II, the binding energy of Al 2p is about 74.6 eV for Al^{3+} ions. Compared to the binding energy of the metal state Al^m atoms, the binding energy of Al 2p electron in the interface has shifted by 1.0 eV towards the higher side. The Al^{3+} ions are primarily attributed to the dissolution of the aluminium oxide on the composite surface (Seen Fig. 3). During bonding composite-bismuthate glass, the Al_2O_3 was dissolved in the glass up to its saturation point due to the presence of the sufficient oxide film (2-3 μm), and the mutual solubility between the glass and the aluminium oxide on the composite formed the interface which was saturated with the oxide state Al^{3+} ions.[5] Meanwhile, the localized Al_2O_3 layer disappeared due to the fast diffusion rate for Al^{3+} ions[5], causing that SiC particles and the matrix were brought into direct contact with the molten glass. Therefore, a weak bond of the van der Waals type between SiC particles and the glass was produced (See Fig. 6b). At the same time, the redox reactions may be occurred between the matrix and the oxide present in the glass. In Region III, the binding energy of the Al 2p in the oxide state Al^{3+} ions is 74.4 eV. The oxide state Al^{3+} ions found in the glass is resulted from the diffusion of aluminium oxide during bonding. It should to be noted that compared to the position of the Al 2p peak in Region II, the binding energy of Al 2p electron in the glass has shifted by 0.2 eV towards the minus direction. It may be ascribed to the incorporation of Al_2O_3 into the glass. The incorporation of Al_2O_3 into the glass changed in the original structure of the glass and enhanced the polarization of the glass, and resulting in the fluctuation of Al 2p peak position toward the lower energy.[24, 25]

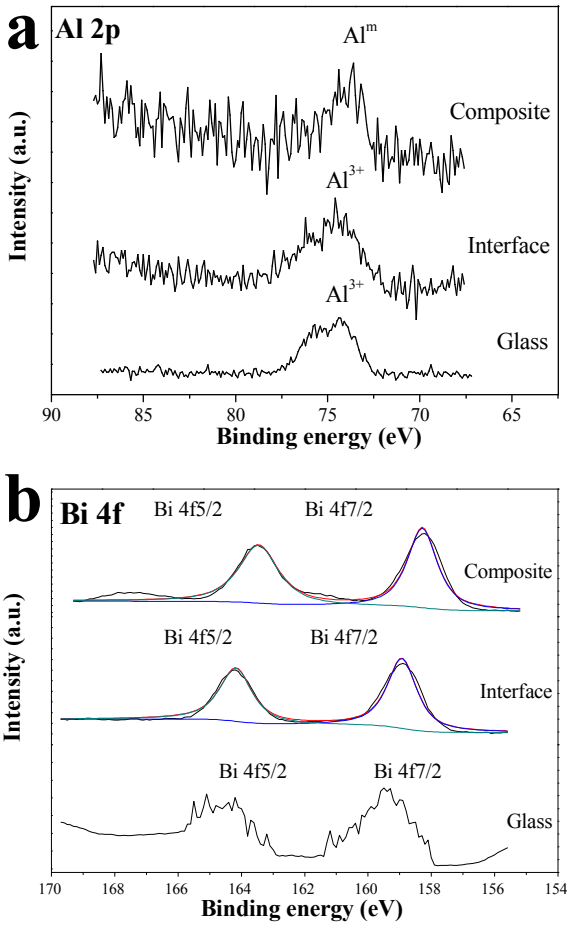

Figure 7XPS high-resolution spectrum of (a) the Al, (b) the Bi.

The photoelectron spectra of the Bi bands obtained from the three regions of the joint is shown in Fig. 7b. In Region III, the Bi4f XPS spectrum presents two peaks with a binding energy of 159.1 eV for Bi $4f_{7/2}$ and 165.1 eV for Bi $4f_{5/2}$, implying the presence of Bi atoms in two different chemical states.[26] In Region II, the Bi 4f spectrum was fitted through Gaussian decomposition by two peaks: the Bi $4f_{7/2}$ peak at 158.8 eV and the Bi $4f_{5/2}$ peak at 164.1 eV. The position of the Bi $4f_{7/2}$ peaks is in good agreement with that of the Bi ions reported in the literature[23], indicating the existence of glassy phase within the interface. The result reveals that the strong ionic-covalent bonds were produced at the composite-glass interface which linked the glass to the composite surface.[5] At the same time, the Bi $4f_{5/2}$ peak is identified as the metallic state Bi^m.[23] The result confirms that the redox reactions took place between Bi_2O_3 present in the

glass and the matrix in the local region. The uncompleted orbital Bi 4f ions were reduced due to obtaining the free electrons of the metallic Al atoms. The dendrites of the metallic Bi atoms (See Fig. 5c) precipitated in the interfacial region, and the acted as anchor points between the composite and the glass.[5] The results show that the interface possesses a mixed property of the metal-metal bond and the ionic-covalent bond. In Region I, the curve fitting of the Bi 4f spectrum has been performed and the fitting result coincided with the measured peak morphology. The Bi $4f_{7/2}$ binding energy for Bi^{3+} ions and Bi $4f_{5/2}$ binding energy for the metallic Bi^m atoms were determined by fitting the spectral line. The measured Bi $4f_{7/2}$ binding energy is 157.8 eV for Bi^{3+} ions and Bi $4f_{5/2}$ binding energy is 164.1 eV for the metallic Bi^m atoms, respectively. These values are good agreement with those present in the literature.[23] The Bi^{3+} ions in the composite are related to severe corrosion of the glass. The metallic Bi^m atoms in the composite are resulted from the diffusion of Bi^m atoms, contributing to the formation of the Bi-Bi bonding and the Bi-Al bonding between the interface and the composite.[5] The spectra results of the Al and Bi can be confirmed each other, indicating the occurrence of redox reactions. For the glass containing Bi_2O_3 bonded to the composite, the following reactions are believed to occur:

$$Al^0 - 3e^- \rightarrow Al^{3+} \quad (4)$$

$$Bi^{3+} + 3e^- \rightarrow Bi \quad (5)$$

Conclusions

1. A glass with compositions of $72.7Bi_2O_3$-$15B_2O_3$-10BaO-$2.3Li_2O$ was developed. Its melting point was lower than the melting temperature of the iron intermetallics in the 70 vol.% SiC_p/Al composite, and its thermal expansion coefficient matched with that of the composite. The glass can meet the requirements of the composite-glass bonding.

2. The composite-glass material was prepared by bonding glass-SiC_p/Al composite at 565 □ for 20 min in air. The FEGSEM image revealed that the composite-glass material exhibited the good bonding, and the mutual diffusion between the glass and the composite formed an interface layer with about 2 μm in thickness. The shear strength of the composite-glass material reached 5.34 MPa. The p-v surface error of the polished composite-glass material achieved 0.05λ at 632.8-nm.

3. The XPS investigations revealed the existence of the chemical shifts of the Al2p and Bi4f binding energies in the composite-glass material. During bonding, the glass has also gradually adjusted its properties to match the matrix properties by the interface, and a strong chemical bond at the interface was resulted from the incorporation the oxide film on the composite surface into the glass. The metallic bonding of the matrix was gradually substituted for the ionic-covalent bonding of the glass within the interface. In the local region, the Bi ions in the glass gained the free electrons from the Al metal atoms of the composite, forming the precipitates of Bi atoms on the composite surface.

Acknowledgements

This study was funded by the School of Mechanical and Automotive Engineering. All investigations were performed in the laboratory at South China University of Technology called advanced metallic materials processing.

Notes and references

1. S. W. Guo, G. Y. Zhang, L. B. Li, W. Y. Wang and X. Z. Zhao, Mater Design, 2009, 30, 9-14.
2. Y. M. Zhang, J. H. Zhang, J. C. Han, X. D. He and W. Yao, Mater Lett, 2004, 58, 1204-1208.
3. R. S. Breidenthal, R. GalatSkey and J. J. Geany, P Soc Photo-Opt Ins, 1995, 2543, 248-253.
4. L. B. Li, M. Z. An and G. H. Wu, Appl Surf Sci, 2005, 252, 959-965.
5. I. W. Donald, J Mater Sci, 1993, 28, 2841-2886.
6. J. Wang, M. Y. Su, J. Q. Qi and L. Q. Chang, Sensor Actuat B-Chem, 2009, 139, 418-424.
7. P. C. Xie, P. He, Y. C. Yen, K. J. Kwak, D. Gallego-Perez, L. Q. Chang, W. C. Liao, A. Yi and L. J. Lee, Surf Coat Tech, 2014, 258, 174-180.
8. C. Lara, M. J. Pascual, R. Keding and A. Durán, Journal of Power Sources, 2006, 157, 377-384.
9. Z. Li, A. M. Samuel, F. H. Samuel, C. Ravindran, S. Valtierra and H. W. Doty, Mat Sci Eng a-Struct, 2004, 367, 96-110.
10.C. Chanmuang, M. Naksata, T. Chairuangsri, H. Jain and C. E. Lyman, Mat Sci Eng a-Struct, 2008, 474, 218-224.
11.Y. W. Li, W. B. Zhang, I. F. Hsieh, G. L. Zhang, Y. Cao, X. P. Li, C. Wesdemiotis, B. Lotz, H. M. Xiong and S. Z. D. Cheng, J Am Chem Soc, 2011, 133, 10712-10715.
12.X. Gong, L. Han, Y. Yue, J. Gao and C. Gao, Journal of colloid and interface science, 2011, 355, 368-373.
13.X. Gong, S. Frankert, Y. J. Wang and L. Li, Chem Commun, 2013, 49, 7803-7805.
14.M. F. Ibrahim, E. Samuel, A. M. Samuel, A. M. A. Al-Ahmari and F. H. Samuel, Mater Design, 2011, 32, 2130-2142.
15.Y. M. Wu, J. Xiong, R. M. Lai, X. Y. Zhang and Z. X. Guo, J Alloy Compd, 2009, 475, 332-338.
16.A. K. Varshneya, J Am Ceram Soc, 1980, 63, 311-315.
17.M. Hida, Y. Takemoto, Z. Y. Song and M. Sawada, J Mater Sci Lett, 1996, 15, 1669-1673.
18.H. Xiang, L. Guan, Z. Peng and J. Li, Ceramics International, 2014, 40, 4985-4988.

19. D. Q. Lei, Z. F. Wang, J. Li, J. B. Li and Z. J. Wang, Renew Energ, 2012, 48, 85-91.
20. M. Mantel, J Non-Cryst Solids, 2000, 273, 294-301.
21. Eng News-Rec, 1984, 212, 32-32.
22. S. Qu, H. Lou and X. Li, Journal of Composite Materials, 2015, DOI: 10.1177/0021998314568166.
23. B. R. Lawn, B. J. Hockey and H. Richter, J Microsc-Oxford, 1983, 130, 295-308.
24. X. Guo, H. J. Li, L. B. Su, P. S. Yu, H. Y. Zhao, Q. G. Wang, J. F. Liu and J. Xu, Opt Mater, 2012, 34, 675-678.
25. Y. Fujimoto and M. Nakatsuka, J Non-Cryst Solids, 2006, 352, 2254-2258.
26. M. Milanova, R. Iordanova, K. L. Kostov and Y. Dimitriev, J Non-Cryst Solids, 2014, 401, 175-180.